sFigure 1

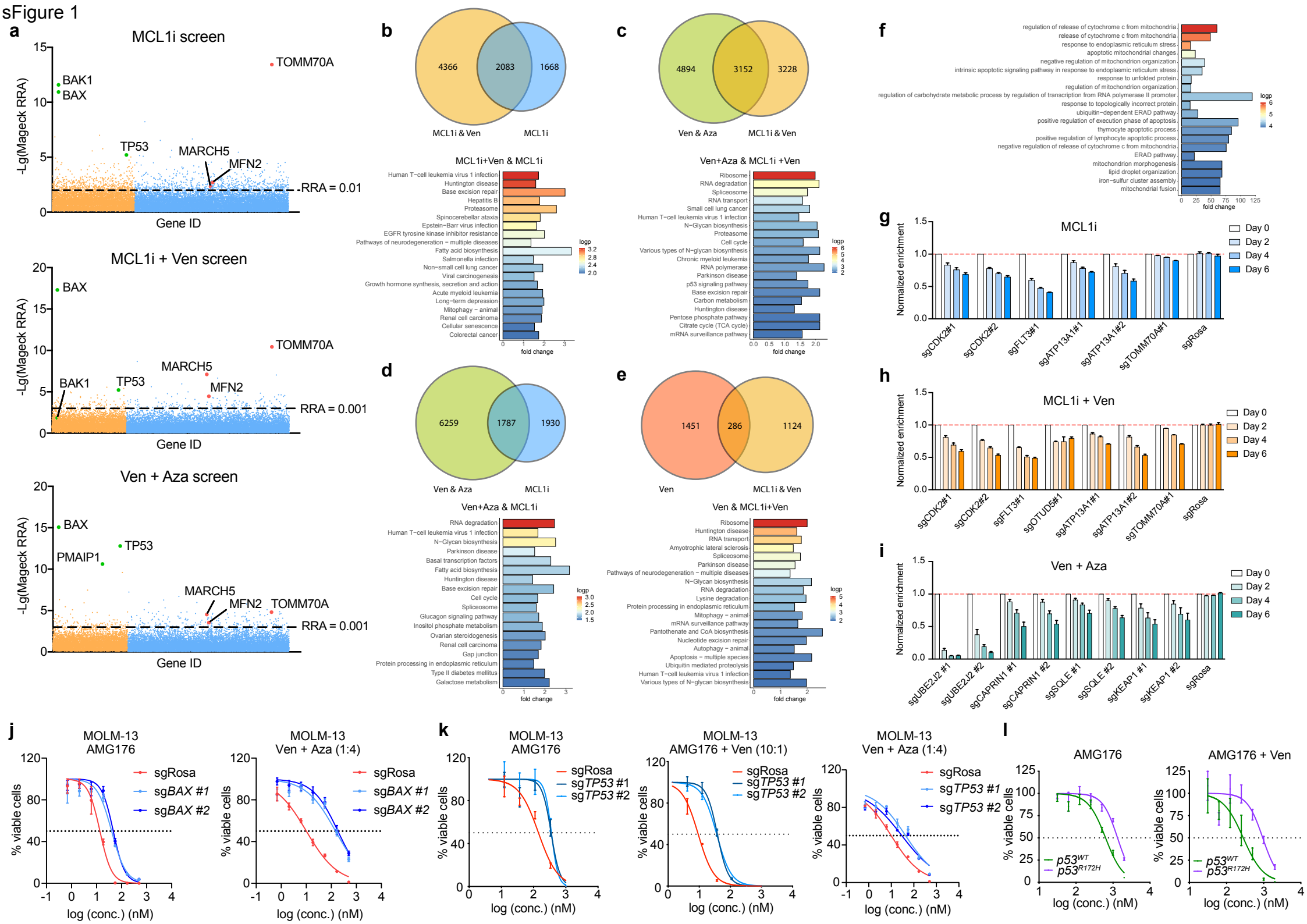
a
MCL1i screen
TOMM70A
BAK1
BAX
TP53
MARCH5
MFN2
RRA = 0.01
-Lg(Mageck RRA)
Gene ID
MCL1i + Ven screen
BAX
TOMM70A
MARCH5
BAK1
TP53
MFN2
RRA = 0.001
Ven + Aza screen
BAX
TP53
PMAIP1
MARCH5
MFN2
TOMM70A
RRA = 0.001
b
4366
2083
1668
MCL1i & Ven
MCL1i
MCL1i+Ven & MCL1i
Human T-cell leukemia virus 1 infection
Huntington disease
Base excision repair
Hepatitis B
Proteasome
Spinocerebellar ataxia
Epstein-Barr virus infection
EGFR tyrosine kinase inhibitor resistance
Pathways of neurodegeneration - multiple diseases
Fatty acid biosynthesis
Salmonella infection
Non-small cell lung cancer
Viral carcinogenesis
Growth hormone synthesis, secretion and action
Acute myeloid leukemia
Long-term depression
Mitophagy - animal
Renal cell carcinoma
Cellular senescence
Colorectal cancer
logp
fold change
c
4894
3152
3228
Ven & Aza
MCL1i & Ven
Ven+Aza & MCL1i +Ven
Ribosome
RNA degradation
Spliceosome
RNA transport
Small cell lung cancer
Human T-cell leukemia virus 1 infection
N-Glycan biosynthesis
Proteasome
Cell cycle
Various types of N-glycan biosynthesis
Chronic myeloid leukemia
RNA polymerase
Parkinson disease
p53 signaling pathway
Base excision repair
Carbon metabolism
Huntington disease
Pentose phosphate pathway
Citrate cycle (TCA cycle)
mRNA surveillance pathway
logp
fold change
d
6259
1787
1930
Ven & Aza
MCL1i
Ven+Aza & MCL1i
RNA degradation
Human T-cell leukemia virus 1 infection
N-Glycan biosynthesis
Parkinson disease
Basal transcription factors
Fatty acid biosynthesis
Huntington disease
Base excision repair
Cell cycle
Spliceosome
Glucagon signaling pathway
Inositol phosphate metabolism
Ovarian steroidogenesis
Renal cell carcinoma
Gap junction
Protein processing in endoplasmic reticulum
Type II diabetes mellitus
Galactose metabolism
logp
fold change
e
1451
286
1124
Ven
MCL1i & Ven
Ven & MCL1i+Ven
Ribosome
Huntington disease
RNA transport
Amyotrophic lateral sclerosis
Spliceosome
Parkinson disease
Pathways of neurodegeneration - multiple diseases
N-Glycan biosynthesis
RNA degradation
Lysine degradation
Protein processing in endoplasmic reticulum
Mitophagy - animal
mRNA surveillance pathway
Pantothenate and CoA biosynthesis
Nucleotide excision repair
Autophagy - animal
Apoptosis - multiple species
Ubiquitin mediated proteolysis
Human T-cell leukemia virus 1 infection
Various types of N-glycan biosynthesis
logp
fold change
f
regulation of release of cytochrome c from mitochondria
release of cytochrome c from mitochondria
response to endoplasmic reticulum stress
apoptotic mitochondrial changes
negative regulation of mitochondrion organization
intrinsic apoptotic signaling pathway in response to endoplasmic reticulum stress
response to unfolded protein
regulation of mitochondrion organization
regulation of carbohydrate metabolic process by regulation of transcription from RNA polymerase II promoter
response to topologically incorrect protein
ubiquitin-dependent ERAD pathway
positive regulation of execution phase of apoptosis
thymocyte apoptotic process
positive regulation of lymphocyte apoptotic process
negative regulation of release of cytochrome c from mitochondria
ERAD pathway
mitochondrion morphogenesis
lipid droplet organization
iron-sulfur cluster assembly
mitochondrial fusion
logp
fold change
g
MCL1i
Normalized enrichment
Day 0
Day 2
Day 4
Day 6
sgCDK2#1
sgCDK2#2
sgFLT3#1
sgATP13A1#1
sgATP13A1#2
sgTOMM70A#1
sgRosa
h
MCL1i + Ven
Normalized enrichment
Day 0
Day 2
Day 4
Day 6
sgCDK2#1
sgCDK2#2
sgFLT3#1
sgOTUD5#1
sgATP13A1#1
sgATP13A1#2
sgTOMM70A#1
sgRosa
i
Ven + Aza
Normalized enrichment
Day 0
Day 2
Day 4
Day 6
sgUBE2J2 #1
sgUBE2J2 #2
sgCAPRIN1 #1
sgCAPRIN1 #2
sgSQLE #1
sgSQLE #2
sgKEAP1 #1
sgKEAP1 #2
sgRosa
j
MOLM-13
AMG176
% viable cells
sgRosa
sgBAX #1
sgBAX #2
log (conc.) (nM)
MOLM-13
Ven + Aza (1:4)
% viable cells
sgRosa
sgBAX #1
sgBAX #2
log (conc.) (nM)
k
MOLM-13
AMG176
% viable cells
sgRosa
sgTP53 #1
sgTP53 #2
log (conc.) (nM)
MOLM-13
AMG176 + Ven (10:1)
% viable cells
sgRosa
sgTP53 #1
sgTP53 #2
log (conc.) (nM)
MOLM-13
Ven + Aza (1:4)
% viable cells
sgRosa
sgTP53 #1
sgTP53 #2
log (conc.) (nM)
l
AMG176
% viable cells
p53WT
p53R172H
log (conc.) (nM)
AMG176 + Ven
% viable cells
p53WT
p53R172H
log (conc.) (nM)

Supplemental Figure 1. Integration of CRISPR/Cas9 loss-of-function screens to identify dependencies and liabilities in BH3-mimetics treatments.

a. Manhattan plots of MCL1i (top), MCL1i+Ven (middle) and Ven+Aza (bottom) screens in MOLM-13 cells. The positive hits are highlighted in orange, while the negative hits are shown in blue.

b-e. Venn diagrams (top) and KEGG gene set enrichment analyses (bottom) of the significantly selected genes falling in the corresponding intersection of the pairwise screens comparisons. Data for the Ven (Venetoclax) monotherapy are from our previously published screen[5].

f. Gene ontology (GO) enrichment analysis of the commonly selected genes in all three screens.

g-i. Competition-based viability assays in MOLM-13 cells treated with AMG176 (g), AMG176+Ven (h), or Ven+Aza (i).

j. Dose-response curves of MOLM-13 cells infected with sgRNAs targeting BAX or Rosa, and treated with increasing doses of AMG176 (left) or Ven+Aza (right).

k. Dose-response curves of MOLM-13 cells infected with sgRNAs targeting TP53 or Rosa, and treated with increasing doses of AMG176 (left), AMG176+Ven (middle) or Ven+Aza (right).

l. Dose-response curves of RN2 ($p53^{WT}$) or KL974 ($p53^{R172H}$) cells treated with increasing doses of AMG176 (left) or AMG176+Ven (right).

Data represent mean ± SD (n=3). The statistical analysis was performed using unpaired two-tailed *t*-test.

sFigure 2

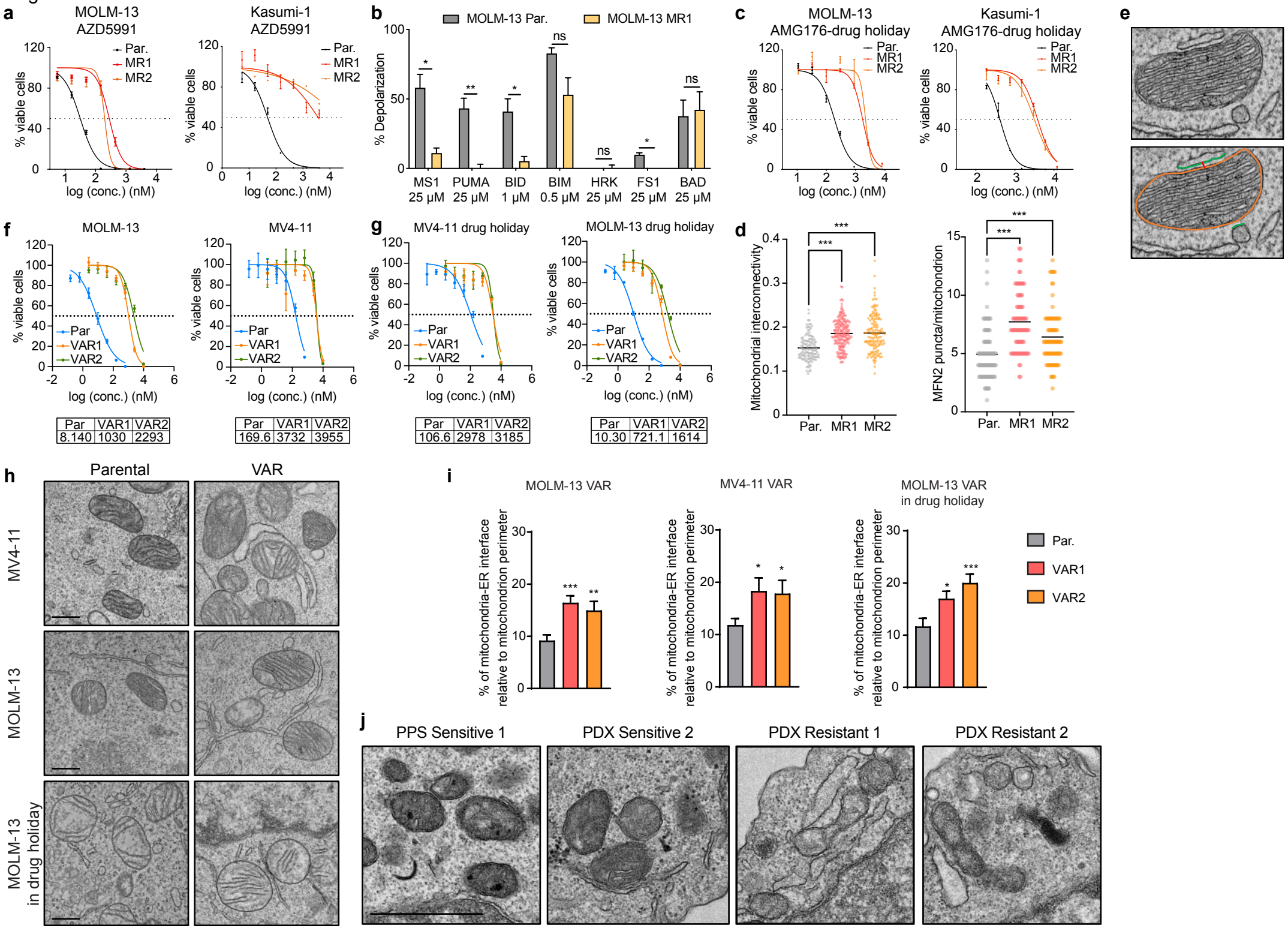
a
MOLM-13
AZD5991
Kasumi-1
AZD5991
Par.
MR1
MR2
% viable cells
log (conc.) (nM)
b
MOLM-13 Par.
MOLM-13 MR1
% Depolarization
MS1 25 µM
PUMA 25 µM
BID 1 µM
BIM 0.5 µM
HRK 25 µM
FS1 25 µM
BAD 25 µM
ns
c
MOLM-13
AMG176-drug holiday
Kasumi-1
AMG176-drug holiday
e
f
MOLM-13
MV4-11
Par
VAR1
VAR2
Par | VAR1 | VAR2
8.140 | 1030 | 2293
169.6 | 3732 | 3955
g
MV4-11 drug holiday
MOLM-13 drug holiday
106.6 | 2978 | 3185
10.30 | 721.1 | 1614
d
Mitochondrial interconnectivity
MFN2 puncta/mitochondrion
h
Parental
VAR
MV4-11
MOLM-13
MOLM-13 in drug holiday
i
MOLM-13 VAR
MV4-11 VAR
MOLM-13 VAR in drug holiday
% of mitochondria-ER interface relative to mitochondrion perimeter
Par.
VAR1
VAR2
j
PPS Sensitive 1
PDX Sensitive 2
PDX Resistant 1
PDX Resistant 2

Supplemental Figure 2. Increased mitochondria-ER interactions contribute to BH3-mimetics resistance.

a. IC_{50} curves of AZD5991 in parental (Par.) or MCL1i-resistant (MR) AML cell lines after 48 hrs treatment (MOLM-13; left, Kasumi-1; right). Data represent mean ± SD (n=3).

b. BH3 profiling in which the percentage of mitochondrial membrane depolarization comparing MOLM-13 parental and MOLM-13 MR1 cells was measured (n=4, mean ± SD). A representative experiment from three independent biological experiments is shown.

c. IC_{50} curves of AMG176 in Par. or MR AML cells after drug holiday (MOLM-13; left, Kasumi-1; right). Data represent mean ± SD (n=3).

d. Quantification of mitochondrial interconnectivity (area/perimeter) and measurement of MFN2 puncta per individual mitochondrion in MOLM-13 cells from super-resolution imaging.

e. Schematic of an electron micrograph illustrating mitochondria-ER contacts quantified in this study. The mitochondrion perimeter is colored in orange. In red we denote the mitochondrion-ER distance, and in green we illustrate the interface of ER in close apposition to the mitochondrion.

f. IC_{50} curves of Ven+Aza in Par. or VAR AML cells after 48 hrs treatment (MV4-11; left, MOLM-13; right). Data represent mean ± SD (n=3). IC50 values are in nM.

g. IC_{50} curves of Ven+Aza in Par. or VAR AML cells after drug holiday (MV4-11; left, MOLM-13; right). Data represent mean ± SD (n=3). IC50 values are in nM.

h. Representative electron micrographs of mitochondria and ER from parental or VAR MV4-11 and MOLM-13 cells. Scale bars represent 0.5 μm.

i. Quantification of mitochondria-ER contacts in experiments described in (g). Data represent mean ± SEM.

j. Representative electron micrographs of mitochondria and ER from blasts of primary and xenografted patient samples. Scale bar represents 1 μm. PPS: primary patient sample.

The statistical analysis was performed using unpaired two-tailed *t*-test.

sFigure 3

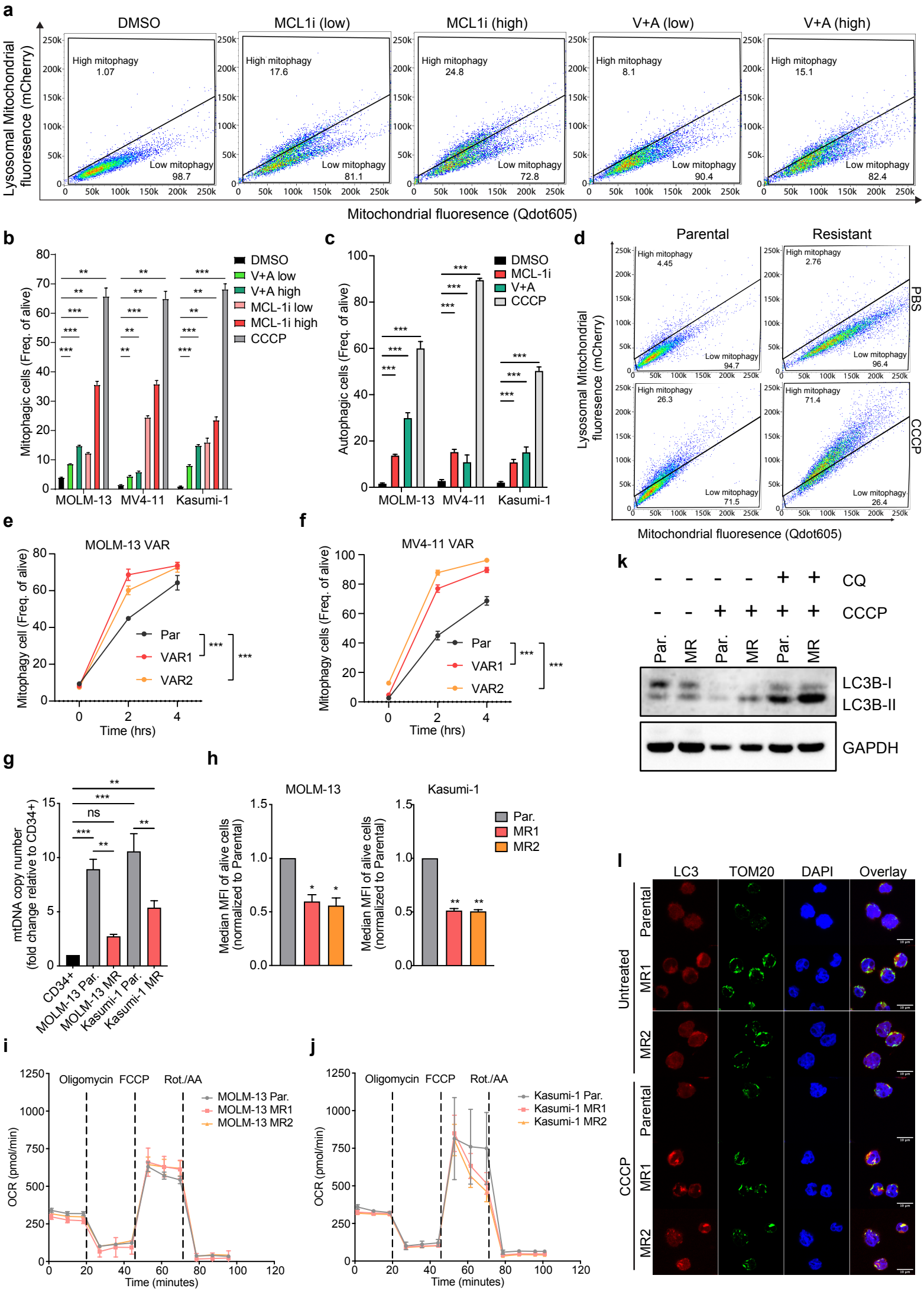
a
DMSO
MCL1i (low)
MCL1i (high)
V+A (low)
V+A (high)
High mitophagy 1.07
Low mitophagy 98.7
High mitophagy 17.6
Low mitophagy 81.1
High mitophagy 24.8
Low mitophagy 72.8
High mitophagy 8.1
Low mitophagy 90.4
High mitophagy 15.1
Low mitophagy 82.4
Lysosomal Mitochondrial fluoresence (mCherry)
Mitochondrial fluoresence (Qdot605)
b
Mitophagic cells (Freq. of alive)
DMSO
V+A low
V+A high
MCL-1i low
MCL-1i high
CCCP
MOLM-13
MV4-11
Kasumi-1
c
Autophagic cells (Freq. of alive)
DMSO
MCL-1i
V+A
CCCP
MOLM-13
MV4-11
Kasumi-1
d
Parental
Resistant
PBS
CCCP
High mitophagy 4.45
Low mitophagy 94.7
High mitophagy 2.76
Low mitophagy 96.4
High mitophagy 26.3
Low mitophagy 71.5
High mitophagy 71.4
Low mitophagy 26.4
Lysosomal Mitochondrial fluoresence (mCherry)
Mitochondrial fluoresence (Qdot605)
e
MOLM-13 VAR
Mitophagy cell (Freq. of alive)
Par
VAR1
VAR2
Time (hrs)
f
MV4-11 VAR
Mitophagy cells (Freq. of alive)
Par
VAR1
VAR2
Time (hrs)
k
CQ
CCCP
Par.
MR
LC3B-I
LC3B-II
GAPDH
g
mtDNA copy number (fold change relative to CD34+)
CD34+
MOLM-13 Par.
MOLM-13 MR
Kasumi-1 Par.
Kasumi-1 MR
h
MOLM-13
Kasumi-1
Median MFI of alive cells (normalized to Parental)
Par.
MR1
MR2
l
LC3
TOM20
DAPI
Overlay
Untreated
CCCP
Parental
MR1
MR2
i
Oligomycin
FCCP
Rot./AA
OCR (pmol/min)
MOLM-13 Par.
MOLM-13 MR1
MOLM-13 MR2
Time (minutes)
j
Oligomycin
FCCP
Rot./AA
OCR (pmol/min)
Kasumi-1 Par.
Kasumi-1 MR1
Kasumi-1 MR2
Time (minutes)

Supplemental Figure 3. Mitophagy affects the responsiveness of AML cells to BH3-mimetics.

a. Representative flow cytometry plots showing Qdot 605 fluorescence (mitochondria in the cytosol, physiological pH 8.0) versus mCherry fluorescence (mitochondria within the lysosomes, acidic pH 4.5) from mitoKeima-expressing Kasumi-1 cells treated with BH3 mimetics for 16 hrs. MCL1i (AMG176) low: 700 nM; MCL1i (AMG176) high: 1800 nM; V+A (venetoclax+azacytidine) low: 400 nM+1600 nM; V+A (venetoclax+azacytidine) high: 800 nM+3200 nM.

b. Bar plots depicting the frequency of alive, mitoKeima-expressing AML cells undergoing mitophagy upon BH3 mimetics treatment for 16 hrs (n=3, mean ± SD).
MOLM-13 MCL1i (AMG176) low: 400 nM; MCL1i (AMG176) high: 1000 nM; V+A low: 10+40 nM; V+A high: 40+160 nM;
MV4-11 MCL1i (AMG176) low: 500 nM; MCL1i (AMG176) high: 1500 nM; V+A low: 40+160 nM; V+A high: 100+400 nM;
Kasumi-1 MCL1i (AMG176) low: 700 nM; MCL1i (AMG176) high: 1800 nM; V+A low: 400+1600 nM; V+A high: 800+3200 nM.
CCCP: 10 μM for all cell lines.

c. Bar plots depicting the frequency of alive, LC3-GFP-mCherry-expressing AML cells undergoing autophagy upon drug treatment for 21 hrs (n=3, mean ± SD). MCL1i (AMG176): 1 μM; V+A: (MOLM-13) 40 nM+160 nM; V+A (MV4-11): 100 nM+400 nM; V+A (Kasumi-1): 400 nM+1600 nM. CCCP: 10 μM.

d. Representative flow cytometry plots showing Qdot 605 fluorescence (mitochondria in the cytosol, physiological pH 8.0) versus mCherry fluorescence (mitochondria within the lysosomes, acidic pH 4.5) from parental or resistant mitoKeima-expressing Kasumi-1 cells treated with 15 μM CCCP or PBS for 2 hrs.

e-f. Frequency of mitophagic cells in a time-course of CCCP treatment (10 μM) in MOLM-13 VAR cells (e) and MV4-11 VAR cells (f). Data represent mean ± SD (n=3).

g. Quantification of mtDNA content in Parental and MR cells relative to CD34+ cells in healthy cord blood (n=3, mean ± SEM).

h. Mitochondrial mass quantification based on the mean fluorescent intensity (MFI) of mitoTracker Green FM in MOLM-13 MR and parental cells (left), as well as in Kasumi-1 MR and parental cells (right) (n=3, mean ± SEM).

i-j. Seahorse analyses of sensitive and resistant clones from MOLM-13 (i) and Kasumi-1 (j) (n=6, mean ± SD).
MOLM-13: Oligomycin 1 μM, FCCP 2 μM, and Rotenone/Antimycin 0.5 μM.
Kasumi-1: Oligomycin 1 μM, FCCP 1 μM, and Rotenone/Antimycin 0.5 μM.

k. Immunoblotting for the autophagy marker LC3B in MOLM-13 treated with CCCP (10 μM) for 30 min with or without chloroquine (CQ, 50 μM) for 3 hrs.

l. Representative confocal images of MOLM-13 Parental and MR cells ectopically expressing LC3-mCherry, treated with CCCP, and stained for TOM20 (green; mitochondria) and DAPI (Blue; DNA). CCCP treatment leads to the formation of LC3 puncta onto mitochondria. Scale bars represent 10 μm.

The statistical analysis was performed using unpaired two-tailed *t*-test.

sFigure 4

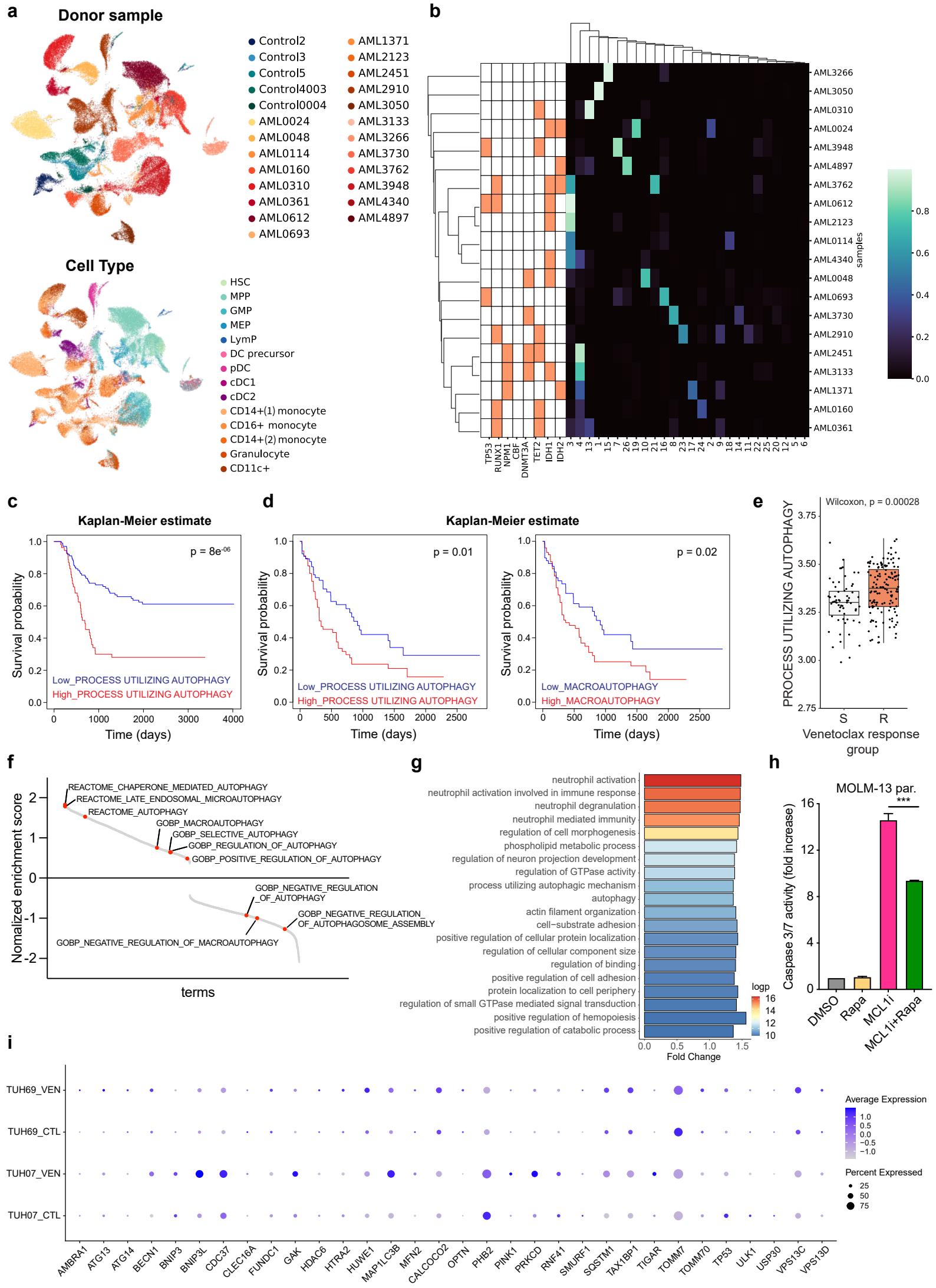
a
Donor sample
Control2
Control3
Control5
Control4003
Control0004
AML0024
AML0048
AML0114
AML0160
AML0310
AML0361
AML0612
AML0693
AML1371
AML2123
AML2451
AML2910
AML3050
AML3133
AML3266
AML3730
AML3762
AML3948
AML4340
AML4897
Cell Type
HSC
MPP
GMP
MEP
LymP
DC precursor
pDC
cDC1
cDC2
CD14+(1) monocyte
CD16+ monocyte
CD14+(2) monocyte
Granulocyte
CD11c+
b
samples
TP53
RUNX1
NPM1
CBF
DNMT3A
TET2
IDH1
IDH2
c
Kaplan-Meier estimate
p = 8e-06
Survival probability
Low_PROCESS UTILIZING AUTOPHAGY
High_PROCESS UTILIZING AUTOPHAGY
Time (days)
d
Kaplan-Meier estimate
p = 0.01
Low_PROCESS UTILIZING AUTOPHAGY
High_PROCESS UTILIZING AUTOPHAGY
Time (days)
p = 0.02
Low_MACROAUTOPHAGY
High_MACROAUTOPHAGY
Time (days)
e
Wilcoxon, p = 0.00028
PROCESS UTILIZING AUTOPHAGY
S
R
Venetoclax response group
f
Nomalized enrichment score
REACTOME_CHAPERONE_MEDIATED_AUTOPHAGY
REACTOME_LATE_ENDOSOMAL_MICROAUTOPHAGY
REACTOME_AUTOPHAGY
GOBP_MACROAUTOPHAGY
GOBP_SELECTIVE_AUTOPHAGY
GOBP_REGULATION_OF_AUTOPHAGY
GOBP_POSITIVE_REGULATION_OF_AUTOPHAGY
GOBP_NEGATIVE_REGULATION_OF_AUTOPHAGY
GOBP_NEGATIVE_REGULATION_OF_AUTOPHAGOSOME_ASSEMBLY
GOBP_NEGATIVE_REGULATION_OF_MACROAUTOPHAGY
terms
g
neutrophil activation
neutrophil activation involved in immune response
neutrophil degranulation
neutrophil mediated immunity
regulation of cell morphogenesis
phospholipid metabolic process
regulation of neuron projection development
regulation of GTPase activity
process utilizing autophagic mechanism
autophagy
actin filament organization
cell−substrate adhesion
positive regulation of cellular protein localization
regulation of cellular component size
regulation of binding
positive regulation of cell adhesion
protein localization to cell periphery
regulation of small GTPase mediated signal transduction
positive regulation of hemopoiesis
positive regulation of catabolic process
logp
Fold Change
h
MOLM-13 par.
***
Caspase 3/7 activity (fold increase)
DMSO
Rapa
MCL1i
MCL1i+Rapa
i
TUH69_VEN
TUH69_CTL
TUH07_VEN
TUH07_CTL
AMBRA1
ATG13
ATG14
BECN1
BNIP3
BNIP3L
CDC37
CLEC16A
FUNDC1
GAK
HDAC6
HTRA2
HUWE1
MAP1LC3B
MFN2
CALCOCO2
OPTN
PHB2
PINK1
PRKCD
RNF41
SMURF1
SQSTM1
TAX1BP1
TIGAR
TOMM7
TOMM70
TP53
ULK1
USP30
VPS13C
VPS13D
Average Expression
Percent Expressed

Supplemental Figure 4. Enhanced autophagic clearance of mitochondria as a mechanism of resistance to BH3-mimetics in AML.

a. Uniform Manifold Approximation and Projection (UMAP) of AML malignant cells of 20 adult AML patients (top) and healthy hematopoietic stem/progenitor and myeloid cells from 5 healthy donors colored by annotated cell type (bottom).

b. Heat map showing the usage of each of the 25 non-negative matrix factorization (NMF) gene expression profiles (GEP) in each patient and their associated mutations. Note GEP 4 corresponds to the Autophagy feature.

c. Kaplan-Meier curves split by high/low mean gene expression of the 'Process using autophagy' GO pathway genes overlapping with autophagy GEP using overall survival (OS) as an endpoint in TARGET-AML cohort. Split points were determined using rpart. Log rank test was used to determine significance.

d. Kaplan-Meier curves split by high/low mean gene expression of the 'Process using autophagy' and 'Macroautophagy' GO pathway genes overlapping with autophagy GEP using overall survival (OS) as an endpoint in TCGA-LAML cohort. Split points were determined using rpart. Log rank test was used to determine significance.

e. Boxplot of 'Process using autophagy' scores in Venetoclax sensitive and resistant patients from the BeatAML cohort. Wilcoxon rank sum test was used to determine significance. Box plots represent the median with the box bounding the interquartile range (IQR) and whiskers showing the most extreme points within 1.5× IQR.

f. Waterfall plot depicting gene set enrichment analysis of genes differentially expressed in venetoclax-resistant (IC_{50} > 0.25 μM) vs. venetoclax-sensitive (IC_{50} < 0.25 μM) patients of the TUH cohort[6].

g. GO pathway analysis of the top significantly differentially expressed genes in Kasumi-1 MR cells vs Kasumi-1 parental cells.

h. Caspase 3/7 assay in MOLM-13 parental cells treated with AZD5991 (MCL1i, 1 μM, 8 hr) and rapamycin (Rapa, 250 nM, 26 hr). Data represent mean ± SEM of three independent biological replicates.

i. Heat map/dot plot showing the differential mRNA expression of mitophagy-related genes in two human PDXs before and after treatment with venetoclax[6]. The color intensity indicates the average gene expression in each cell, while the size of the circle indicates the percentage of cells expressing the corresponding gene.

The statistical analysis was performed using unpaired two-tailed *t*-test.

sFigure 5

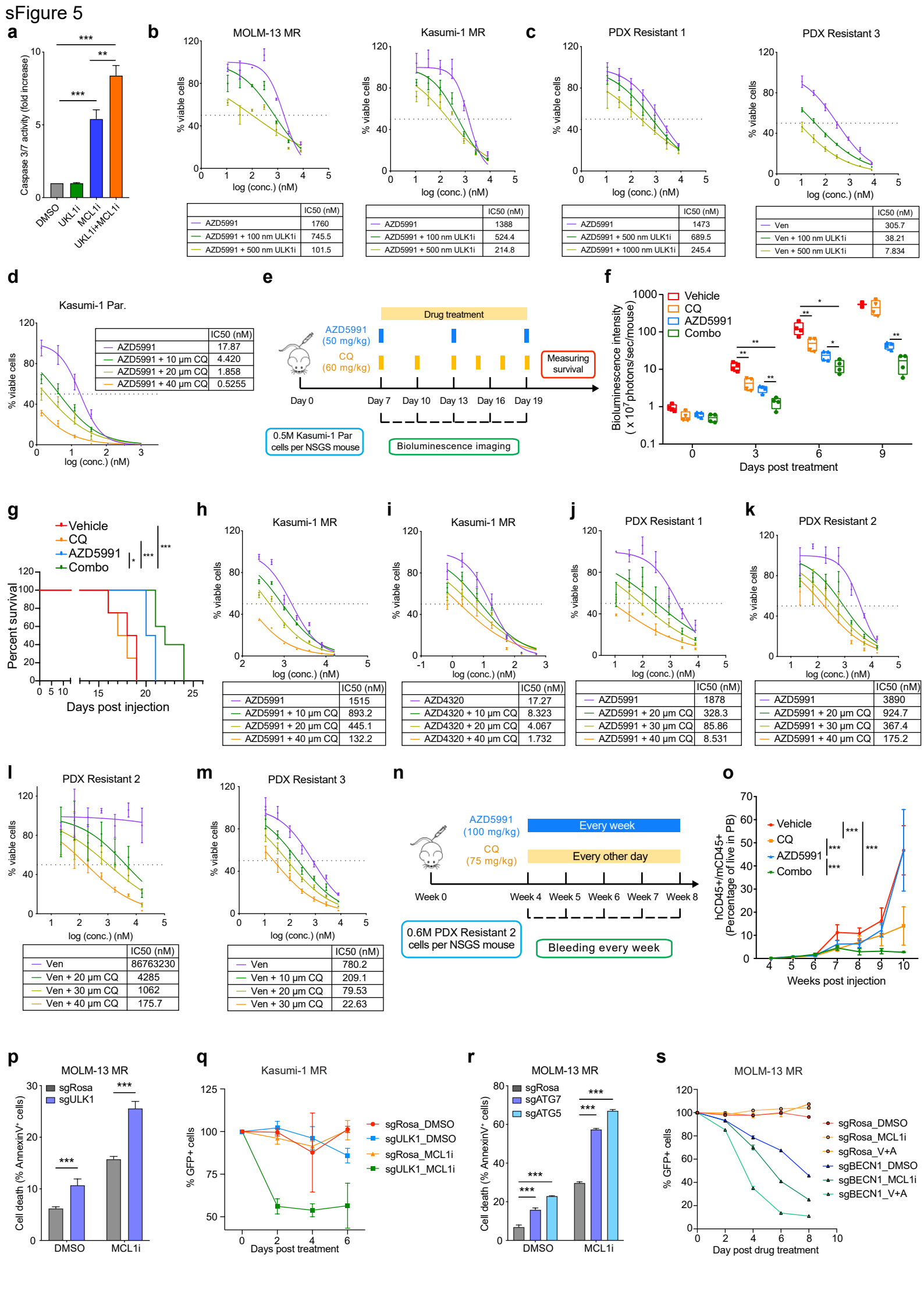
a
Caspase 3/7 activity (fold increase)
DMSO
UKL1i
MCL1i
UKL1i+MCL1i
b
MOLM-13 MR
% viable cells
log (conc.) (nM)
AZD5991 IC50 (nM) 1760
AZD5991 + 100 nm ULK1i 745.5
AZD5991 + 500 nm ULK1i 101.5
Kasumi-1 MR
AZD5991 1388
AZD5991 + 100 nm ULK1i 524.4
AZD5991 + 500 nm ULK1i 214.8
c
PDX Resistant 1
AZD5991 1473
AZD5991 + 500 nm ULK1i 689.5
AZD5991 + 1000 nm ULK1i 245.4
PDX Resistant 3
Ven 305.7
Ven + 100 nm ULK1i 38.21
Ven + 500 nm ULK1i 7.834
d
Kasumi-1 Par.
AZD5991 17.87
AZD5991 + 10 μm CQ 4.420
AZD5991 + 20 μm CQ 1.858
AZD5991 + 40 μm CQ 0.5255
e
Drug treatment
AZD5991 (50 mg/kg)
CQ (60 mg/kg)
Measuring survival
Day 0
Day 7
Day 10
Day 13
Day 16
Day 19
0.5M Kasumi-1 Par cells per NSGS mouse
Bioluminescence imaging
f
Vehicle
CQ
AZD5991
Combo
Bioluminescence intensity (x 10^7 photons/sec/mouse)
Days post treatment
g
Vehicle
CQ
AZD5991
Combo
Percent survival
Days post injection
h
Kasumi-1 MR
AZD5991 1515
AZD5991 + 10 μm CQ 893.2
AZD5991 + 20 μm CQ 445.1
AZD5991 + 40 μm CQ 132.2
i
Kasumi-1 MR
AZD4320 17.27
AZD4320 + 10 μm CQ 8.323
AZD4320 + 20 μm CQ 4.067
AZD4320 + 40 μm CQ 1.732
j
PDX Resistant 1
AZD5991 1878
AZD5991 + 20 μm CQ 328.3
AZD5991 + 30 μm CQ 85.86
AZD5991 + 40 μm CQ 8.531
k
PDX Resistant 2
AZD5991 3890
AZD5991 + 20 μm CQ 924.7
AZD5991 + 30 μm CQ 367.4
AZD5991 + 40 μm CQ 175.2
l
PDX Resistant 2
Ven 86763230
Ven + 20 μm CQ 4285
Ven + 30 μm CQ 1062
Ven + 40 μm CQ 175.7
m
PDX Resistant 3
Ven 780.2
Ven + 10 μm CQ 209.1
Ven + 20 μm CQ 79.53
Ven + 30 μm CQ 22.63
n
AZD5991 (100 mg/kg)
Every week
CQ (75 mg/kg)
Every other day
Week 0
Week 4
Week 5
Week 6
Week 7
Week 8
0.6M PDX Resistant 2 cells per NSGS mouse
Bleeding every week
o
Vehicle
CQ
AZD5991
Combo
hCD45+/mCD45+ (Percentage of live in PB)
Weeks post injection
p
MOLM-13 MR
sgRosa
sgULK1
Cell death (% AnnexinV+ cells)
DMSO
MCL1i
q
Kasumi-1 MR
% GFP+ cells
sgRosa_DMSO
sgULK1_DMSO
sgRosa_MCL1i
sgULK1_MCL1i
Days post treatment
r
MOLM-13 MR
sgRosa
sgATG7
sgATG5
Cell death (% AnnexinV+ cells)
DMSO
MCL1i
s
MOLM-13 MR
% GFP+ cells
sgRosa_DMSO
sgRosa_MCL1i
sgRosa_V+A
sgBECN1_DMSO
sgBECN1_MCL1i
sgBECN1_V+A
Day post drug treatment

Supplemental Figure 5. Synergism between BH3-mimetics and macroautophagy inhibition in human AML.

a. Caspase 3/7 assay in MOLM-13 MR1 cells treated with AZD5991 (MCL1i, 1 μM, 8 hrs) and ULK1i (500 nM, 11 hrs). Data represent mean ± SEM of three independent biological replicates.

b. Dose-response curves of AZD5991 from MOLM-13 (left) and Kasumi-1 (right) resistant clones with increasing concentrations of ULK1i. Treatments were performed for 24 hrs (n=3, mean ± SD) before viability measurements using Cell Titer Glo.

c. Dose-response curves of AZD5991 (left) or venetoclax (Ven, right) from PDX resistant 1 and 3 with increasing concentrations of ULK1i. Treatments were performed for 24 hrs (n=3, mean ± SD) before viability measurements using Cell Titer Glo.

d. Dose-response curves of AZD5991 from Kasumi-1 parental cells with increasing concentrations of CQ. Treatments were performed for 48 hrs (n=3, mean ± SD) before viability measurements using Cell Titer Glo.

e. Schematic outline of the in vivo experiment using parental Kasumi-1 xenografts.
Mice were transplanted with $0.5x10^6$ GFP/Luciferase-expressing Kasumi-1 cells.
Mice were administrated weekly with AZD5991 or CQ or their combination (Combo) or Vehicle.
Bioluminescent imaging was performed at the indicated time points to measure tumor burden.
Survival was measured at the end of the experiment.

f. Quantification of bioluminescence emitted from the whole body of each mouse described in (e) at the indicated time points.

g. Kaplan-Meier survival curves of MOLM-13 leukemia recipient mice in experiments as in Fig. S5e. The p-values were determined using the Log-rank Mantel-Cox test.

h-i. Dose-response curves of AZD5991 (h) or AZD4320 (i) with increasing concentrations of CQ from Kasumi-1 MR cells. Treatments were performed for 48 hrs before viability measurements using Cell Titer Glo (n=3, mean ± SD).

j-k. Dose-response curves of AZD5991 with increasing concentrations of CQ from patient-derived xenografted cells. Treatments in all PDXs were performed for 24 hrs *ex vivo* (n=3, mean ± SD).

l-m. Dose-response curves of venetoclax (Ven) with increasing concentrations of CQ from patient-derived xenografted cells. Treatments in all PDXs were performed for 24 hrs *ex vivo* (n=3, mean ± SD).

n. Schematic outline of the *in vivo* experiment PDX resistant 2. Mice were transplanted with $0.6x10^6$ PDX cells.
Mice were administrated weekly with AZD5991 or CQ or their combination (Combo) or Vehicle.
Bleeding was performed weekly to measure tumor burden.

o. Ratio of human $CD45^+$ cells (donor PDX cells) to mouse $CD45^+$ cells (recipient hematopoietic cells) in the peripheral blood of animals as described in (n) (mean ± SD). Statistics were calculated using two-way ANOVA.

p. Annexin V staining in MOLM-13 resistant cells transduced with sgRNAs targeting ULK1 or Rosa, after treatment with 500 nM AZD5991 (MCL1i) or DMSO for 24 hrs (n=3, mean ± SD). Statistics were calculated using two-way ANOVA.

q. Competition-based viability assays in Kasumi-1 resistant cells (MR1) transduced with sgRNAs targeting ULK1 or control (Rosa) treated with AMG176 or DMSO. Y-axis denotes the GFP+ percentage relative to day 0 of treatment (n=3, mean ± SD).

r. Annexin V staining in MOLM-13 resistant cells transduced with sgRNAs targeting ATG5 or ATG7 or Rosa, after treatment with 800 nM AZD5991 (MCL1i) or DMSO for 24 hrs (n=3, mean ± SD). Statistics were calculated using two-way ANOVA.

s. Competition-based viability assays in MOLM-13 MR cells transduced with sgRNAs targeting BECN1 or Rosa, treated with MCL1i or Ven+Aza.

sFigure 6

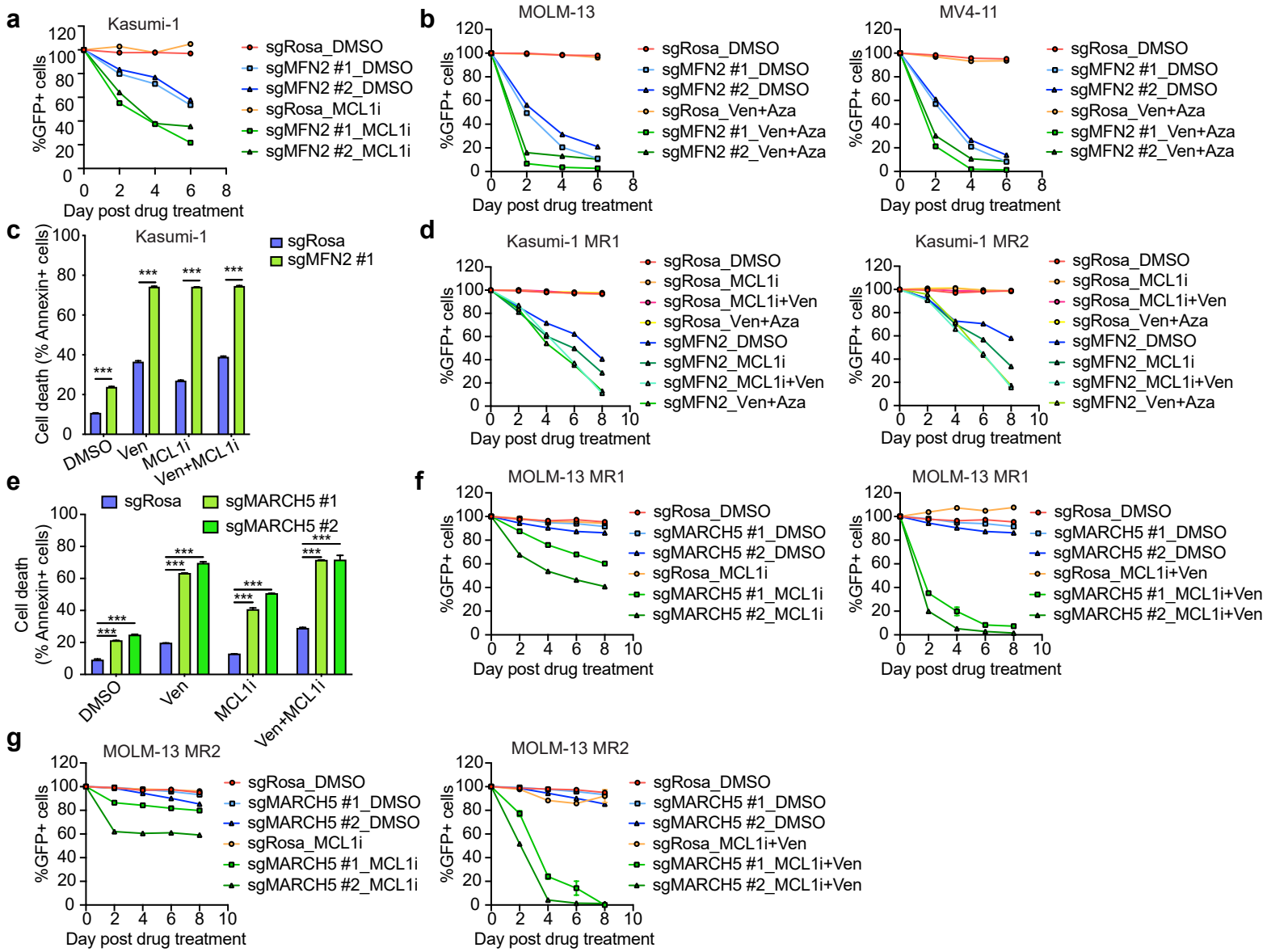

Supplemental Figure 6. Deletion of MFN2 or MARCH5 sensitizes AML cells to BH3-mimetics.

a. Competition-based viability assays in Kasumi-1 transduced with sgRNAs targeting MFN2 or control (Rosa), treated with AMG176.

b. Competition-based viability assays in MOLM-13 (left) and MV4-11 (right) transduced with sgRNAs targeting MFN2 or control (Rosa), treated with Ven+Aza.

c. Annexin V staining in puromycin-selected Kasumi-1 cells transduced with sgRNAs targeting MFN2 or control (Rosa), after treatment with BH3 mimetics or DMSO for 24 hrs.

d. Competition-based viability assays in Kasumi-1 MR1 (left) or MR2 (right) transduced with sgRNAs targeting MFN2 or control (Rosa), treated with AMG176 (MCL1i), AMG176 (MCL1i)+Ven, or Ven+Aza.

e. Annexin V staining in MOLM-13 cells transduced with sgRNAs targeting MARCH5 or control (Rosa), after treatment with BH3 mimetics or DMSO for 24 hrs.

f-g. Competition-based viability assays in MOLM-13 MR1 (f) MOLM-13 MR2 (g) transduced with sgRNAs targeting MARCH5 or control (Rosa), treated with AMG176 (left) or AMG176 + Ven (right).

Data represent mean ± SD (n=3), unless otherwise stated. The statistical analysis was performed using unpaired two-tailed *t*-test.

sFigure 7

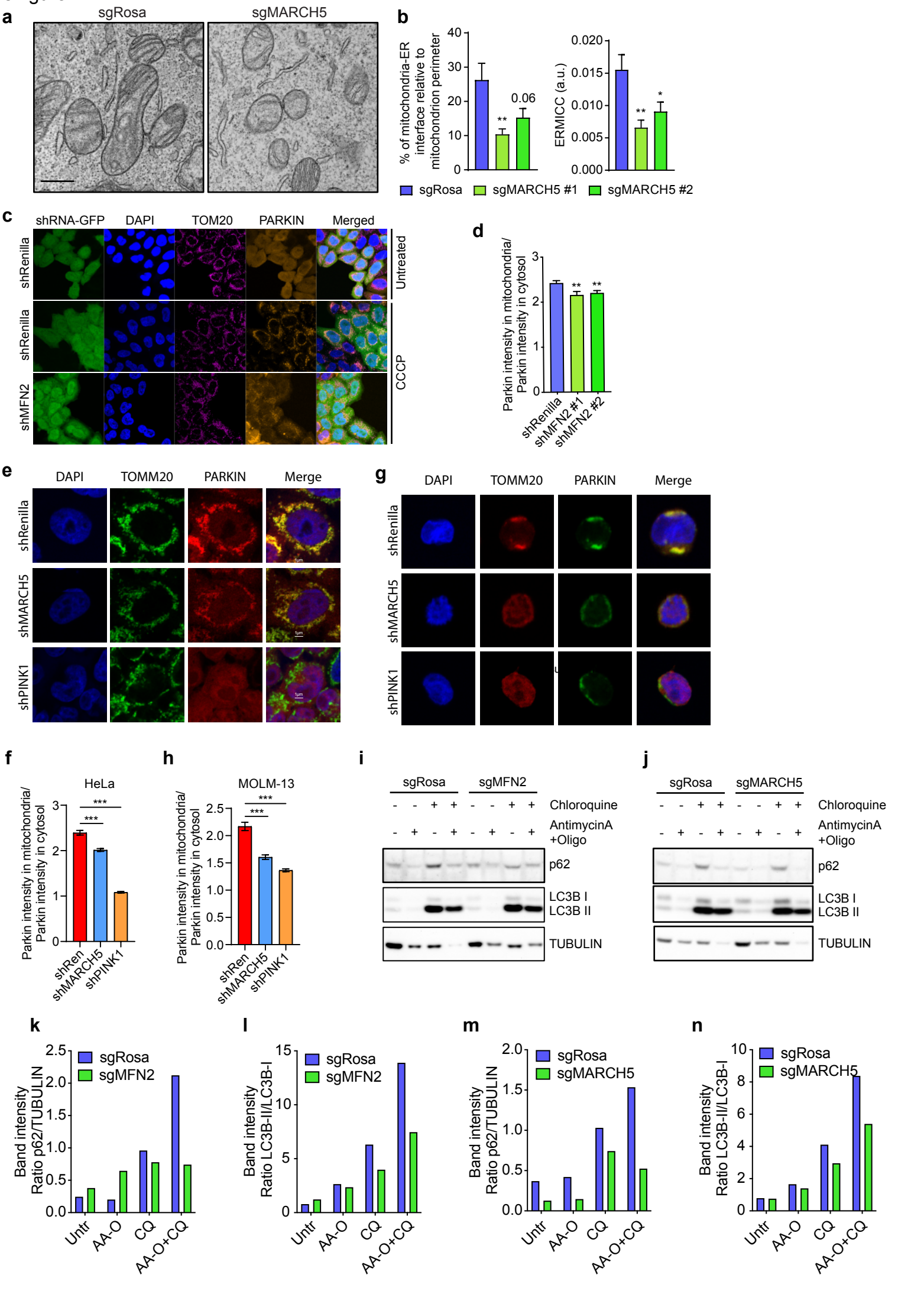
a
sgRosa
sgMARCH5
b
% of mitochondria-ER interface relative to mitochondrion perimeter
40
30
20
10
0
**
0.06
ERMICC (a.u.)
0.020
0.015
0.010
0.005
0.000
**
*
sgRosa
sgMARCH5 #1
sgMARCH5 #2
c
shRNA-GFP
DAPI
TOM20
PARKIN
Merged
shRenilla
shRenilla
shMFN2
Untreated
CCCP
d
Parkin intensity in mitochondria/ Parkin intensity in cytosol
3
2
1
0
**
**
shRenilla
shMFN2 #1
shMFN2 #2
e
DAPI
TOMM20
PARKIN
Merge
shRenilla
shMARCH5
shPINK1
g
DAPI
TOMM20
PARKIN
Merge
shRenilla
shMARCH5
shPINK1
f
HeLa
Parkin intensity in mitochondria/ Parkin intensity in cytosol
3
2
1
0
***
***
shRen
shMARCH5
shPINK1
h
MOLM-13
Parkin intensity in mitochondria/ Parkin intensity in cytosol
2.5
2.0
1.5
1.0
0.5
0.0
***
***
shRen
shMARCH5
shPINK1
i
sgRosa
sgMFN2
- - + + - - + + Chloroquine
- + - + - + - + AntimycinA +Oligo
p62
LC3B I
LC3B II
TUBULIN
j
sgRosa
sgMARCH5
- - + + - - + + Chloroquine
- + - + - + - + AntimycinA +Oligo
p62
LC3B I
LC3B II
TUBULIN
k
Band intensity Ratio p62/TUBULIN
2.5
2.0
1.5
1.0
0.5
0.0
sgRosa
sgMFN2
Untr
AA-O
CQ
AA-O+CQ
l
Band intensity Ratio LC3B-II/LC3B-I
15
10
5
0
sgRosa
sgMFN2
Untr
AA-O
CQ
AA-O+CQ
m
Band intensity Ratio p62/TUBULIN
2.0
1.5
1.0
0.5
0.0
sgRosa
sgMARCH5
Untr
AA-O
CQ
AA-O+CQ
n
Band intensity Ratio LC3B-II/LC3B-I
10
8
6
4
2
0
sgRosa
sgMARCH5
Untr
AA-O
CQ
AA-O+CQ

Supplemental Figure 7. Targeting of MFN2 or MARCH5 impairs the process of mitophagy.

a. Representative electron micrographs of mitochondria and ER from MOLM-13 transduced with sgRNA targeting MARCH5 or control (Rosa). Scale bar represents 0.5 μm.

b. Quantification of the mitochondria-ER contacts in (a). Percentages of mitochondria-ER interface relative to the mitochondrial perimeter (left) and ER-mitochondrial contact coefficient (ERMICC; right) are shown (mean ± SEM).

c. Representative confocal images of PARKIN-mCherry-expressing HeLa cells transduced with the indicated shRNAs (GFP+), treated with CCCP, and stained for TOM20 (mitochondria). Scale bars represent 10 μm.

d. Quantification of PARKIN translocation onto mitochondria (colocalization index of PARKIN on TOM20) relative to the cytosolic PARKIN upon CCCP treatment in experiments as in (c).

e. Representative confocal images of PARKIN-mCherry-expressing HeLa cells transduced with the indicated shRNAs (GFP+), treated with CCCP, and stained for TOM20 (mitochondria). Scale bars represent 1 μm.

f. Quantification of PARKIN translocation onto mitochondria (colocalization index) upon CCCP treatment relative to the cytosolic PARKIN in experiments as in (e).

g. Representative confocal images of PARKIN-mCherry-expressing MOLM-13 cells transduced with the indicated shRNAs (GFP+) and stained for TOM20 (mitochondria). Scale bars represent 2 μm.

h. Quantification of PARKIN translocation onto mitochondria (colocalization index) relative to the cytosolic PARKIN in experiments as in (g).

i-j. Western blot analysis of lysates extracted from Cas9-expressing MOLM-13 cells transduced with the indicated sgRNAs, and treated with Antimycin A + Oligomycin (1 μM /1 μM) and/or chloroquine (100 μM) for 16 hrs.

k. Quantitative densitometric analysis of p62 relative to TUBULIN bands in Western blots as in (i).

l. Quantitative densitometric analysis of LC3B-II relative to LC3B-I bands in Western blots as in (i).

m. Quantitative densitometric analysis of p62 relative to TUBULIN bands in Western blots as in (j).

n. Quantitative densitometric analysis of LC3B-II relative to LC3B-I bands in Western blots as in (j).

Statistics were calculated using unpaired two-tailed *t*-test. Untr: Untreated; AA-O: Antimycin A + Oligomycin; CQ: Chloroquine.